Composites Science and Technology 89 (2013) 44–51

Contents lists available at ScienceDirect

Composites Science and Technology

journal homepage: www.elsevier.com/locate/compscitech

A mesoscale ultrasonic attenuation finite element model of composites with random-distributed voids

Yalin Yu, Jinrui Ye *, Yang Wang, Boming Zhang, Guocheng Qi

School of Materials Science and Engineering, Beihang University, Beijing 100191, China

ARTICLE INFO

Article history:
Received 2 March 2013
Received in revised form 3 September 2013
Accepted 22 September 2013
Available online 29 September 2013

Keywords:
A. Polymer–matrix composites
B. Porosity/voids
Random distribution
C. Finite element analysis (FEA)
D. Ultrasonics

ABSTRACT

Interaction between ultrasonic wave and fiber reinforced composites with voids was investigated on the mesoscale by numerical method in this work. DIGIMAT-FE software was used to establish a mesoscale model of void-containing composites, which revealed the real microstructure with randomly distributed voids. Ultrasonic excitation was loaded into the mesoscale model via ABAQUS/Explicit before the finite element analysis (FEA) was carried out. Take T800 carbon fiber/epoxy composite material as an example, the accuracy of the simulated method was verified by comparing the numerical prediction with the analytical and experimental results. Therefore, this simulation method not only can be an effective guidance for manufacturing process but also provide a theoretical basis for reducing void level in order to increase performance of composites.

© 2013 Elsevier Ltd. All rights reserved.

1. Introduction

Service performance of fiber-reinforced composite is severely influenced by defects introduced from manufacturing process, especially voids [1,2]. Ultrasonic nondestructive testing is considered as the most conventional examination technique for characterizing composite defects and damages on account of its high sensitivity, accuracy and simplicity [3]. Thus, there is a strongly growing need to explore the influence of the voids in composite parts on ultrasonic attenuation during quality evaluation process.

Void size and distribution have significant impacts on the ultrasonic attenuation of composite laminates. A number of studies conducted on the geometry of voids in the composite laminates concluded that the void size and aspect ratio mainly ranged from 0.01 mm to 1 mm and from 1 to 4, respectively [4–6]. The majority of the voids can be considered spherical, except those with large aspect ratio (above 4) [4–6]. In addition, there are different discussions in terms of the void distribution [5,7,8]. However, no well-defined principle has been developed for accurate description.

Due to the periodicity and symmetry of fiber reinforced composites, representative volume element (RVE) of the mesoscale geometric composite structure can be extensively used for the finite element analysis (FEA) in order to study the micro-performance [9–12]. However, numerical model of fiber reinforced composites with the actual volume fraction, shape and spatial distribution of voids within the laminates is rarely reported in literature because traditional modeling approach has a limitation when describing void character.

This investigation managed to take the random features of the voids into consideration by the implementation of DIGIMAT software [13], a nonlinear multi-scale materials and structures modeling platform. The size, spatial distribution and volume fraction of the voids were precisely controlled on mesoscale in this numerical method. Then, in the present work, a mesoscale model of composites with random-distributed voids was successfully built by DIGIMAT-FE. The mesoscale model with void phase effectively reflected the real microstructure and mesoscale properties of the composite material. Five models at each void level (1%, 2% and 3%, respectively) were generated for the randomness and inhomogeneity of void distribution. After applying ultrasonic excitation, the FEA of the mesoscale model was carried out [14]. The ultrasonic attenuations were calculated at different void levels for T800/epoxy composites, and the accuracy of the numerical method was discussed by comparing the simulated prediction with both analytical and experimental results.

2. Experimental procedure

2.1. Preparation of specimens

Square ($300 \times 300\ mm^2$) panels of 5 mm nominal thickness were made of T800/epoxy prepreg (a product of CYTEC Industries) by autoclave processing following the quasi-isotropic stacking sequence. The prepreg was cured at 185 °C for 3 h and all the heating

* Corresponding author. Tel./fax: +86 1082338756.
E-mail address: jinrui_ye@126.com (J. Ye).

0266-3538/$ - see front matter © 2013 Elsevier Ltd. All rights reserved.
http://dx.doi.org/10.1016/j.compscitech.2013.09.006

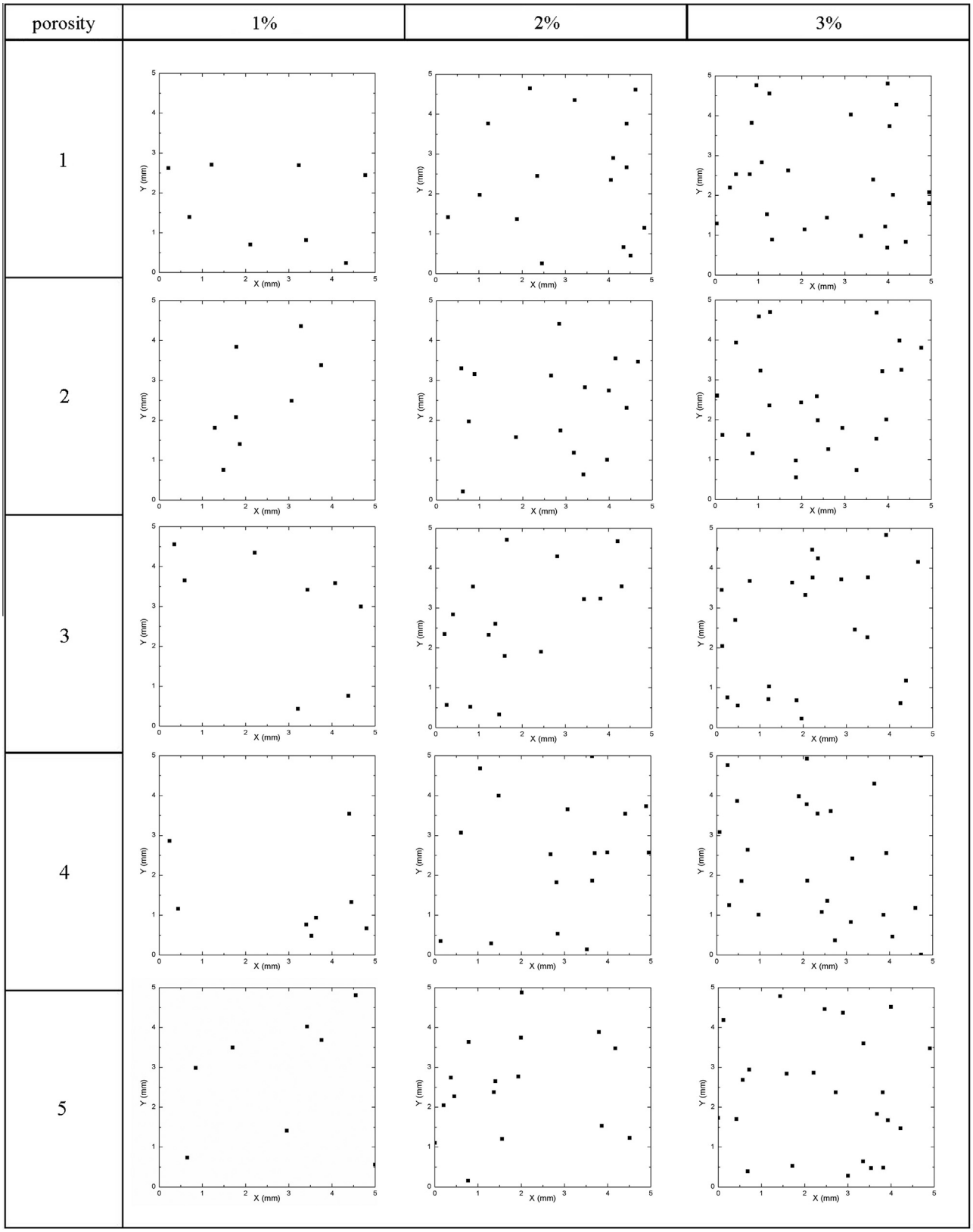

Fig. 1. The void positions of each RVE model at different void levels.

and cooling ramps were carried out at the same rate of 2.5 °C/min. Laminates with intentionally different void levels were produced under an autoclave pressure range of 0.1–0.5 MPa. The pressure inside the vacuum bag was kept 0 MPa throughout the entire cycle.

2.2. C-scan ultrasonic inspection

The ultrasonic attenuation coefficient was measured with ultrasonic echo immersion bottom reflection technique. A glass plane

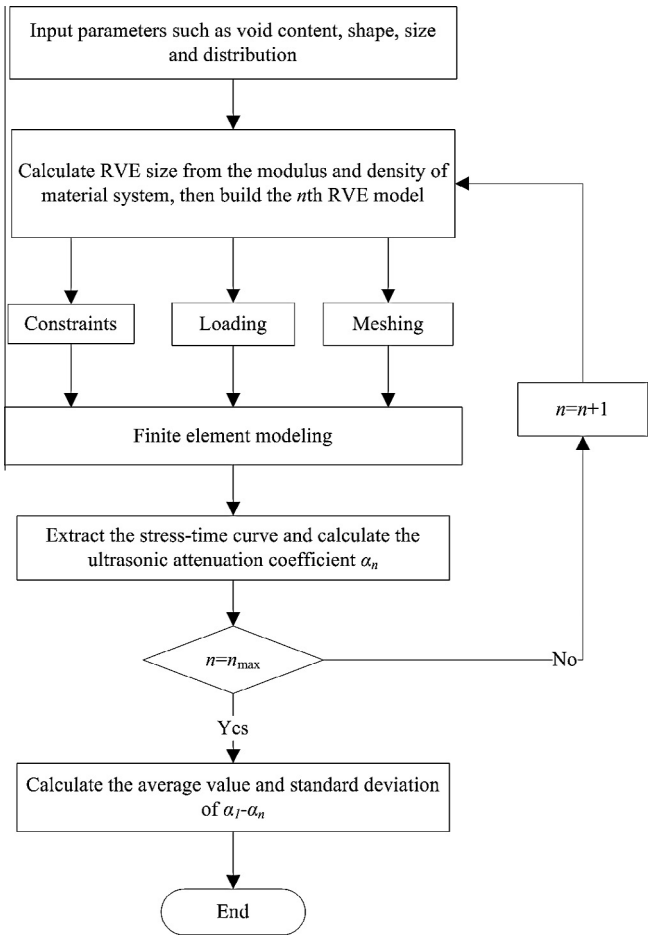

Fig. 2. Flow chart of mesoscale ultrasonic attenuation finite element modeling of composite with voids.

was placed under the sample to enhance the testing sensitivity and separate the ultrasonic back echoes. A flat immersion probe was transported by GE-USIP40 ultrasonic flaw detector that generated a c-scan signal record of the plate with the frequency of 5 MHz. Then a quantized map was drawn to represent different attenuation level changes of the sample.

Attenuation calculations were taken using the equation below on the selected areas of the composite panels.

$$\alpha = \frac{n - m + \log 80/x}{2d} \tag{1}$$

In the equation, α (dB/mm) is the ultrasonic attenuation coefficient of the picked point, d (mm) is the thickness of the plate, n (dB) and m (dB) are the signal gains when there is a sample and otherwise, and x is the extracted amplitude value. The average value of the ultrasonic attenuation coefficients in the selected area stands for the ultrasonic attenuation coefficient of the sample.

2.3. Void content measurement

After c-scan inspection, specimens were cut from the center of each laminate and the void content was measured according to the ASTM D2734-09 and ASTM D2584-11. To have a better assessment of void distribution and shape, the cross-sections of some specimens were polished to achieve a high quality surface. The images were all captured and saved by VHX-900 optical microscope.

3. Numerical method

3.1. Numerical modeling by DIGIMAT

As a finite element based homogenization software which is used to model the multi-physics nonlinear behavior, DIGIMAT-FE is of full ability to generate a realistic RVE of composite microstructures. In addition, the size, position and distribution of composite constituents could also be defined by means of parameter adjustment. As a result, it is quite easy to overcome the difficulty in describing void characters.

Based on the previous surveys [4–8], the assumptions are made in the numerical model that all voids are spherical with a diameter of 100 μm and distributed at random. Random 2D method is taken for void generation to save computing time and improve model efficiency [13]. In this method, random orientation tensor, a = diag (1/2, 1/2, 0), is specified in the (1, 2)-plane. DIGIMAT-FE uses random placement techniques to place the voids one after another in the RVE. The placement of each void results from the convergence of an iterative process. The position of the void is accepted once all constraints on the void position are verified. If the iterative process requires more than the specified maximum number of attempts for random placement, DIGIMAT-FE will stop the generation process after issuing an error message.

However, the numerical model processed by DIGIMAT-FE presents only one state under fixed void content, size and distribution. Therefore, the number of modeling at the same void level ought to be increased to a certain extent to acquire more states, which depends on the computing accuracy needed. Consequently, five models with the same input and different void positions were built up, as shown in Fig. 1.

3.2. Finite element analysis approach

Ultrasonic wave pertains to longitudinal stress wave, which is generated with high frequency and acts on the testing samples in the form of cyclic pressure. Ultrasonic pressure is the pressure change on the node after loading the stress wave on sample. Therefore, the whole process can be transformed into the interaction between stress wave and the elements in medium, which can be simulated through explicit dynamic analysis.

The explicit dynamics analysis procedure in ABAQUS/Explicit is based upon the implementation of an explicit integration rule together with the use of diagonal or "lumped" element mass matrices [14]. The equations of motion for the body are integrated using the explicit central difference integration rule. The explicit procedure integrates through time by using many small time increments. ABAQUS/Explicit uses an adaptive algorithm to determine conservative bounds for the highest element frequency. An estimate of the highest eigenvalue in the system can be obtained by determining the maximum element dilatational mode of the mesh. The stability limit based upon this highest element frequency is conservative in that it will give a smaller stable time increment than the true stability limit that is based upon the maximum frequency of the entire model. The stability limit Δt_{stable} can be rewritten as:

$$\Delta t_{stable} = \frac{Le}{C} \tag{2}$$

where Le is the characteristic element dimension and C is the current effective, dilatational wave speed of the material.

As mentioned in Section 3.1, the established RVE model represents the microstructure of cross-section perpendicular to the fiber-direction which is the symmetry plane of composites. Besides, the length of the composite laminate along the fiber direction is extremely longer than the side length of the RVE model.

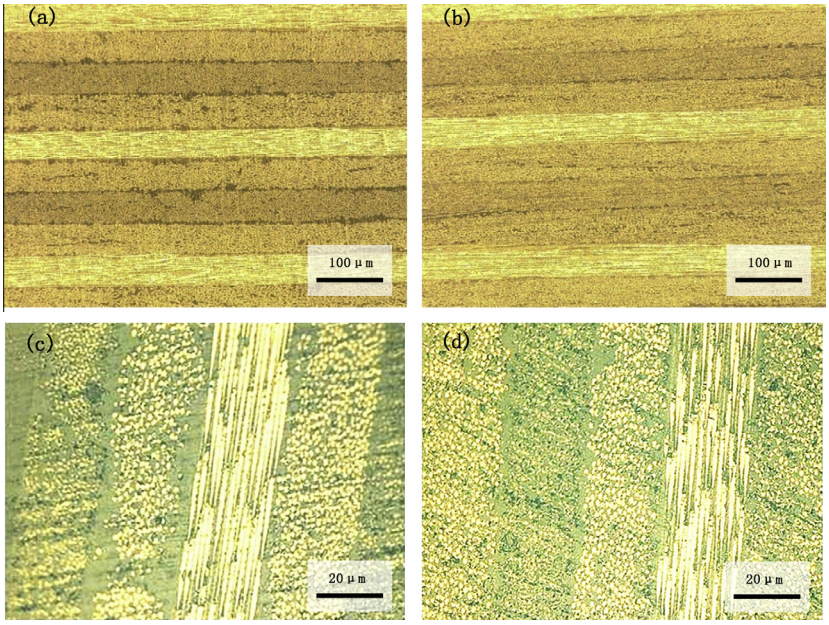

Fig. 3. Micrographs of autoclave processed laminates conditioned under different cure pressures (a) $P = 0.5$ MPa, (b) $P = 0.1$ MPa, (c) $P = 0.5$ MPa, and (d) $P = 0.1$ MPa.

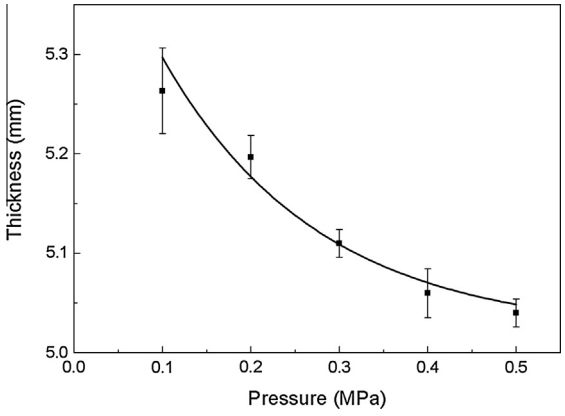

Fig. 4. Thickness of T800/epoxy composite laminates as a function of cure pressure.

Moreover, the load is applied evenly on the laminates along the thickness direction. As mentioned above, the RVE models are under plane-strain state. Wave speed C is a basic property of material which is determined by the module E and density ρ $\left(C = \sqrt{\frac{E}{\rho}}\right)$. The characteristic element dimension Le should be adjusted to about 10 times of wavelength so that the meshes are accurate enough to capture the generated details.

$$Le = \frac{C}{10f} \tag{3}$$

It is appropriate to set the RVE size L to twice of wavelength at least for the same reason that the ultrasonic attenuation can be captured.

$$L \geqslant \frac{2C}{f} \tag{4}$$

The material properties of T800/epoxy void-free composite laminate for numerical modeling were obtained from the experiments and given as follows:

$\rho = 1.54\ \mathrm{g/cm^3}$, $E_1 = 195$ GPa, $E_2 = 8.58$ GPa, $v_{12} = 0.345$, $v_{21} = 0.425$, $G_{12} = 4.57$ GPa.

where E_1, E_2 are the longitudinal and transverse moduli respectively, ρ is the weight density, v_{12} is the major Poisson's ratio, v_{21} is the minor Poisson's ratio, G_{12} is the in-plane shear modulus.

To ensure the stability and convergence in explicit dynamics analysis, the numerical model was established with mesh size of 0.03 mm and RVE size of 5 mm. Additionally, the whole resulting algorithm was briefly summarized in Fig. 2.

4. Results and discussion

4.1. Experimental results

The results of matrix digestion experiment in Section 2.3 showed that the void content varied from 0.12% to 2.57% with the change of the cure pressure. More detailed void characters in fiber reinforced composites were studied with an optical microscope by observing the cross-section of T800/Epoxy samples. Void distributions in composite laminates under different cure pressure are shown in Fig. 3. It is clear that cure pressure has a significant influence on the void size and shape. Moreover, the thickness of the resin-rich regions between the layers increases with the decrease of the cure pressure, as shown in Fig. 3.

The laminate thickness range measured with vernier caliper is plotted in Fig. 4. There was a continual reduction of the thickness until the cure pressure reached roughly 0.4 MPa. Grunenfelder and Nutt [15] also found that the laminate thickness dropped with the decrease of void content, which was due to the volume brought in by voids.

It is well known that there are two ways to form voids. For one thing, gas (volatiles) evolution during cure is the cause of small voids in many resin systems, which is affected little by pressure variation. For another, air bubble trapped in manufacturing process strongly alters with pressure [17, 18]. When the cure pressure increases, it has a larger driving force to remove these trapped voids from high viscosity resin system [5] and limits the trapped void growth [17], which leads to smaller void content and volume.

The distinctions between the laminates at different void levels can also be revealed by ultrasonic C-scanning, as shown in Fig. 5. The red area represents region with lower attenuation, and the

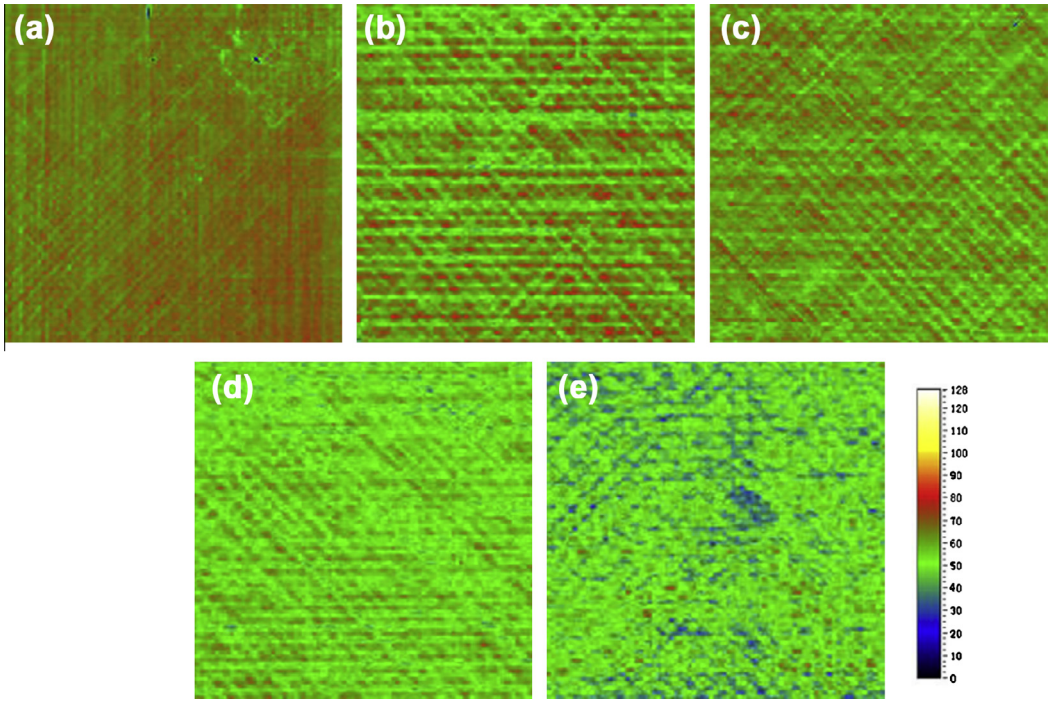

Fig. 5. C-scan showing areas with different void contents (a) Pv = 0.12%, (b) Pv = 1.17%, (c) Pv = 1.36%, (d) Pv = 1.98%, and (e) Pv = 2.29%.

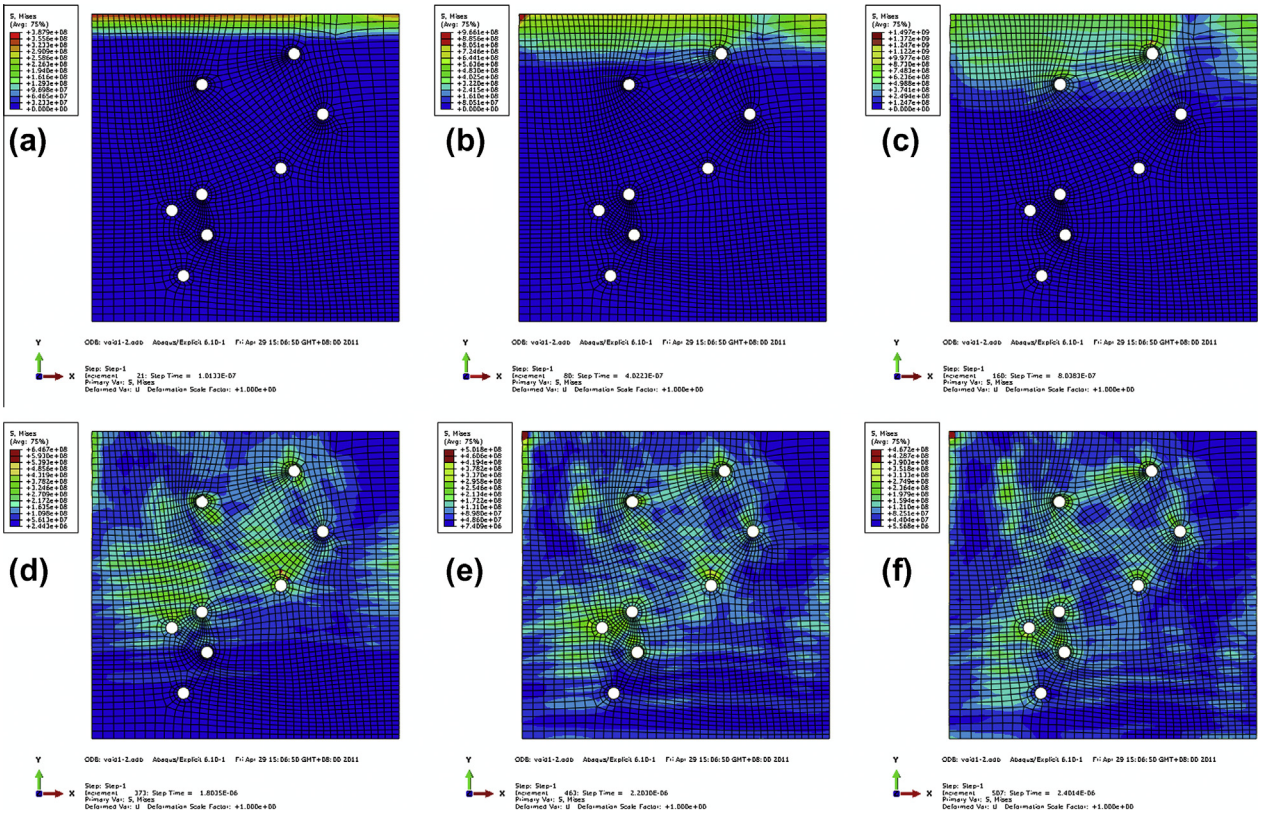

Fig. 6. Acoustic propagation of T800/epoxy composites with a void content of 1% (a) t = 0.10 μs, (b) t = 0.40 μs, (c) t = 0.80 μs, (d) t = 1.80 μs, (e) t = 2.20 μs, and (f) t = 2.40 μs.

blue area represents region with higher attenuation. The quality of composite laminates is dependent on the degree of color uniformity. A composite laminate with larger void content has a more irregular color distribution, in terms of the diversity of void shape, size and location.

The acquirement of ultrasonic attenuation coefficient normally starts with the extraction of echo amplitude data from the central area of the examined composite laminate, where the void content is measured afterwards. Ultrasonic attenuation coefficient of the examined laminate is calculated based upon the Eq. (1), and the

standard deviation (SD) of calculated values in this area is regarded as the error of the ultrasonic attenuation coefficient at this void level. The relationship between void content and ultrasonic attenuation of T800/epoxy composite laminates acquired in the experiments is summarized in Fig. 7(b). The attenuation rises exponentially with the improvement of the void content, and the SD of the attenuation shows an escalating trend as well. A fitting curve was formed and expressed as $\alpha_e = 0.499P_V^2 + 2.30$, where α_e (dB/mm) was the total experimental ultrasonic attenuation coefficient of fiber reinforced composites.

4.2. Finite element analysis of the numerical model

Fig. 6 presents a typical ultrasonic propagation process of composite laminates with a void content of 1%, and the simulating procedure was carried out as shown in Fig. 2. The stress wave started from upper boundary of the model, and had reflections and scatters when reaching the void edge which was set as a free boundary. The reflected waves continued to move forward and met another void edge, which resulted in new reflections and scatters. The stress wave front changed with time like water ripples. The reflected wave continuously propagated and a complicated acoustic field formed eventually.

In this work, five models at the same void level were built to take the effect of random distribution into consideration. Fig. 1 reveals the random but inhomogeneous void distributions in each RVE model with the black spot representing the center of void. In each model the information of distances between every two nearest spots can be gathered by DIGIMAT-FE, and the SD of these data represents the character of void distribution to some extent. Each SD of numerical model at different void levels was calculated and the ultrasonic attenuation coefficients were recorded correspondingly. Fig. 7(a) reveals the numerical relationship which indicates that the ultrasonic attenuation increases with the reduction of SD at the same void content, as well as with the rising of void content at different void levels.

The SD of the distances between every two nearest centers of voids reflects the uniformity of void distribution. A lower SD value of numerical model at the same void content means that the distances between every two void centers have more equal values, which implies a more homogeneous distribution and a longer distance that stress wave propagates. As a consequence, the dissipation and attenuation of energy increased to a certain extent, which makes significant contribution to the decrease in ultrasonic attenuation coefficient.

4.3. Accuracy of the numerical prediction

Before the application of mesoscale finite element model of ultrasonic attenuation, accuracy of the numerical prediction should be validated by comparing with the analytical and experimental methods. The results of three measurements were plotted with void content in Fig. 7(b). To have a better understanding of the prediction deviations, a simple relationship between P_v and α was approximated by the parabola form $\alpha = a + bP_v^2$ [16]. The experimental curve could be expressed as $\alpha = 2.300 + 0.499P_v^2$, and the analytical curve was obtained as $\alpha = 2.326 + 1.168P_v^2$ with a much higher value of curvature. The numerical curve was expressed as $\alpha = 2.255 + 0.272P_v^2$, which had smaller curvature than the experimental one.

The numerical result is lower than the experimental result. The difference between the two attenuation coefficients increases as a function of void content. This may result from the unsmooth surface of the void, which is hard to describe and simulate by software. Therefore, although the void shape is normally assumed to be spherical in order to simplify the void geometry, it is irregular and may cause reduction of the ultrasonic attenuation coefficient. The whole reflected waves are composed of the reflected plane waves and scattering waves. When the stress wave reaches the unsmooth surface of void whose dimension is comparative with the ultrasonic wavelength, distortion of the reflected wave occurs and leads to the scattering effect. Compared with the theoretical smooth surface, the irregularity of void shape engenders much more ultrasonic scatters which results in more energy dispersion in the medium and increases longer propagation distance of reflected plane waves which means an increased ultrasonic absorption induced by internal viscosity. As a consequence, the ultrasonic attenuation coefficients from numerical method are lower than those from experiment.

Moreover, the irregularity level of void distribution rises with the growth of the void content, gives rise to the difference between the numerical and experimental results (shown in Fig. 5). The differences of void characters including size, shape and orientation contribute to the irregular void distribution, whereas it is also hard to describe by software and neglected in numerical modeling. Zhang et al. [19] manifested that the ultrasonic attenuation coefficient had an exponential increase with void size raise. In addition, the influence of void orientation on ultrasonic attenuation could be described by an S-shaped curve. What is more, the inequality of the void size distribution arouses more interaction between ultrasonic scattering waves and the nearby voids, which accounts for a greater ultrasonic attenuation.

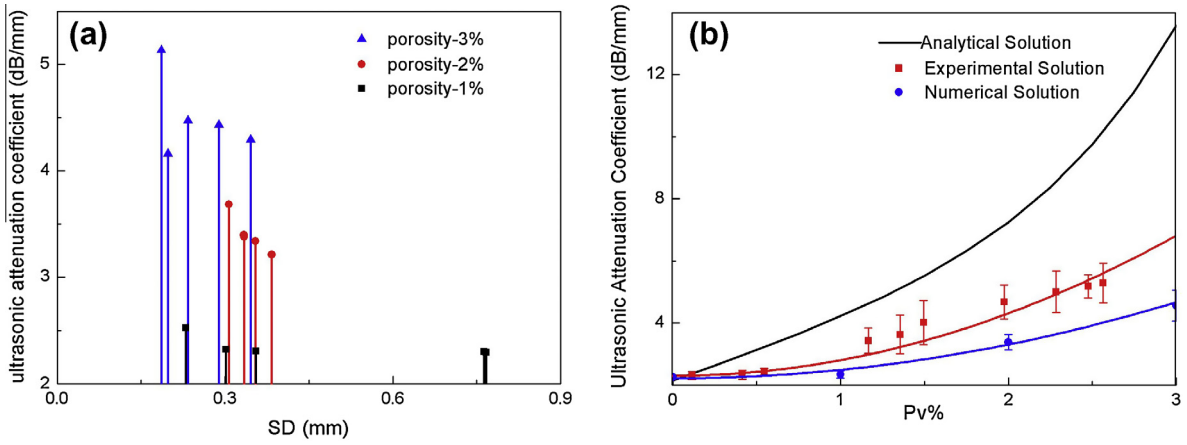

Fig. 7. Predicted ultrasonic attenuation coefficient by numerical method plotted with (a) the standard deviation of distances between every two nearest centers of voids at different void levels, (b) the void content compared with analytical and experimental methods.

In addition, there are microsized voids in composite laminate. They cannot lead to many acoustic scatters and reflections for their dimensions are far smaller than ultrasonic wavelength. While the modulus and density decrease due to the large quantity of such voids, the transmission and dissipation of ultrasonic wave are also affected, as well as the result in further ultrasonic attenuation.

Compared with the analytical method, the numerical prediction is closer to the experimental result under the assumption of the same void size. The numerical result is no more than 30% below the experimental value, while most of the relative errors introduced by analytical method are higher than that from numerical method, with the highest value reaching 90% approximately.

The reasons can be discussed as follows. First of all, comparing the modeling parameters of the two methods, the numerical method requires more material parameter input than analytical method, which means more consideration of the anisotropic properties of composite laminate. It is evident that numerical modeling investigated the interaction between the void-containing composite and ultrasonic wave on the mesoscale. Also, more details of void characterization were introduced to this method. Meanwhile, the assumption proposed by the Martin model [16] that each void scattered independently of the others and they were distributed homogeneously is deviated from practice. Simulation through DIGIMAT-FE can effectively avoid this deviation and realize a better prediction.

In summary, although result for the simulated prediction is lower than the experimental result and beyond the experimental error range, it is an improved and more accurate approach compared with the analytical method.

5. Conclusions

A mesoscale ultrasonic attenuation finite element model of composites with random-distributed voids has been established, taking the randomness of void distribution into consideration. The mesoscale model of void-containing composites built by DIGIMAT-FE effectively reflects the real microstructure and mesoscale material properties of the composites. Ultrasonic excitation was loaded into the mesoscale model via ABAQUS/Explicit, and then the FEA was carried out to simulate the ultrasonic propagation process.

Furthermore, the prediction accuracy of this numerical method has been investigated by comparing it with the analytical and experimental approaches. The simplification of void shape, the neglect of the irregular void distribution and the existence of microsized void are taken into account for the difference between numerical and experimental results. Despite the fact that the result of the simulated prediction is lower than the experimental result and beyond the experimental error range, it still shows advantage in the ultrasonic attenuation prediction compared with the common analytical method. This simulated method can be an effective guidance for manufacturing process and also provide a theoretical basis for reducing void content in order to increase performance of composites.

Appendix A

The analytical prediction of the ultrasonic attenuation of fiber reinforced composites at different void levels was calculated by Martin model [16], which is universally applied. In the model, assumptions were proposed that all voids were spherical and of very nearly the same size and they all had independent scatters and random homogeneous distributions in the medium. On the basis of acoustic analysis, the ultrasonic attenuation coefficient at different void levels was defined as:

$$\alpha = \alpha_b + \frac{8\pi P_V g}{3}\frac{a^3}{\lambda^4} \tag{A1}$$

where α (dB/mm) is the total ultrasonic attenuation coefficient of fiber reinforced composites, α_b (dB/mm) is the ultrasonic attenuation coefficient of void-free fiber reinforced composites, P_V is the void content and a is the diameter of void, λ is the ultrasonic wavelength, and g is an variable dependent written as:

$$g = \frac{4}{3} + 40\frac{2+3\left(\frac{V_L}{V_T}\right)^5}{\left[4-9\left(\frac{V_L}{V_T}\right)^2\right]^2} - \frac{3}{2}\left(\frac{V_L}{V_T}\right)^2 + \frac{2}{3}\left(\frac{V_L}{V_T}\right)^3 + \frac{9}{16}\left(\frac{V_L}{V_T}\right)^4 \tag{A2}$$

where V_L and V_T are the length-wave and shear-wave velocities of fiber-reinforced composites with voids respectively. For acoustic propagation perpendicular to the fiber direction, V_L and V_T are given by

$$V_L = \left(\frac{C_{22}}{\rho}\right)^{1/2} \tag{A3}$$

and

$$V_T = \left(\frac{C_{22}-C_{12}}{2\rho}\right)^{1/2} \tag{A4}$$

where C_{12} and C_{22} are the elastic constants of composites, which are both the functions of void content, resin content and the mechanical properties of the void-free matrix and fibers. The properties of resin matrix and fibers used in the calculations [20] were given as follows:

Fibers: $E_f = 294$ GPa, $G_f = 112$ GPa, $v_f = 0.312$.
Void-free resin: $E_r = 3$ GPa, $G_r = 1.1$ GPa, $v_r = 0.345$.
The analytical calculation was carried out by MATLAB.

References

[1] Almeida SFM. Neto ZdSN. Effect of void content on the strength of composite laminates. Compos Struct 1994;28(2):139–48.
[2] Liu L, Zhang B-M, Wang D-F, Wu Z-J. Effects of cure cycles on void content and mechanical properties of composite laminates. Compos Struct 2006;73(3):303–9.
[3] Mix P. Introduction to nondestructive testing – a training guide. New York: John Wiley & Sons; 1987.
[4] Little JE, Yuan X, Jones MI. Characterisation of voids in fibre reinforced composite materials. NDT and E Int. 2012;46:122–7.
[5] Chambers AR, Earl JS, Squires CA, Suhot MA. The effect of voids on the flexural fatigue performance of unidirectional carbon fibre composites developed for wind turbine applications. Int J Fatigue 2006;28(10):1389–98.
[6] Centea T, Hubert P. Measuring the impregnation of an out-of-autoclave prepreg by micro-CT. Compos Sci Technol 2011;71(5):593–9.
[7] David K, Hsu DK, Kevin M. A morphological study of porosity defects in graphite-epoxy composites. Rev Prog Quantitative NDE 1988;6B:1175–84.
[8] Hernández S, Sket F, Molina-Aldareguía JM, González C, Llorca J. Effect of curing cycle on void distribution and interlaminar shear strength in polymer–matrix composites. Compos Sci Technol 2011;71(10):1331–41.
[9] Xie Q, Li Y-Z, Li B, Li X. The strength prediction of composite laminates based on a quasi-3d finite element models. Sci Technol Eng 2012;13(12):3160–5.
[10] Wu Y, Shivpuri R, Lee LJ. Effect of macro and micro voids on elastic properties of polymer composites. J Reinf Plast Compos 1998;17(15):1391–402.
[11] Huang H, Talreja R. Effects of void geometry on elastic properties of unidirectional fiber reinforced composites. Compos Sci Technol 2005;65(13):1964–81.
[12] Lin L, Chen J, Zhang X, Li X. A novel 2-D random void model and its application in ultrasonically determined void content for composite materials. NDT and E Int 2011;44(3):254–60.
[13] DIGIMAT, 2009. Software Platform for Nonlinear Multi-scale Modeling of Composite Materials and Structures. e-Xstream Engineering, Belgium and Luxembourg. <www.e-Xstream.com>.
[14] Abaqus analysis user's manual, Ver. 6.9. Providence (RI, USA): Dassault Systemes Simulia Corp.; 2009.
[15] Grunenfelder LK, Nutt SR. Void formation in composite prepregs – effect of dissolved moisture. Compos Sci Technol 2010;70(16):2304–9.
[16] Martin BG. Ultrasonic attenuation due to voids in fibre-reinforced plastics. NDT Int 1976;9(5):242–6.

[17] Kardos JL, Duduković MP, Dave R. Void growth and resin transport during processing of thermosetting—matrix composites. In: Dušek K, editor. Epoxy resins and composites IV, vol. 80. Berlin Heidelberg: Springer; 1986. p. 101–23.
[18] Staffan T. Void formation and transport in manufacturing of polymer composites, Maskinteknik/Stomningslara. <www.e-publ.luth.se/avslutade/03488373/184>.
[19] Zhang X, Chen J, Lin L, Li X. Effects on ultrasonic scattering attenuation coefficient of morphological characteristics of voids in composite materials. Chin J Mech Eng 2010;21(14):1735–41.
[20] US Department of Defense. Military handbook–MIL-HDBK-17-1F: composite materials handbook, polymer matrix composites materials properties, vol. 2; 2002.